In-Flow Purification

DOI: 10.1002/ange.201300104

Steady-State Continuous-Flow Purification by Electrophoresis**

*Fletcher J. Agostino, Leonid T. Cherney, Victor Galievsky, and Sergey N. Krylov**

Continuous-flow microsynthesis has a number of important advantages over batch synthesis, namely: increased product yield through atom economy,[1–3] reduced costs associated with starting materials,[4] safer operating conditions,[5,6] high-throughput production by numbering up,[7–9] and automated optimization and control of reaction conditions.[10,11] To fully exploit these advantages, continuous-flow microsynthesis should be supplemented with continuous-flow purification on a compatible scale. Such a combination has not yet been practically realized owing to the lack of a suitable purification technique.[12] Continuous-flow purification can be achieved if a continuous-flow microreactor exits into a wide purification channel in which products are separated in the direction orthogonal to the flow and continuously collected at the exit of the channel. Our recent research efforts have been motivated by understanding that an existing continuous-flow purification technique, free flow electrophoresis (FFE), is naturally suited for combination with continuous-flow microsynthesis in aqueous solution (Figure 1 a).

FFE facilitates continuous separation of molecules in a wide separation channel with a uniform hydrodynamic flow of an electrolyte solution and an electrical field non-parallel (typically orthogonal) to this flow.[13,14] The sample is introduced into the separation channel through a narrow opening as schematically shown in Figure 1 a. Advantageously, FFE devices can be made on a small scale to suit small flow rates used in continuous-flow microsynthesis.[15] Unfortunately, small-scale FFE cannot be used for steady-state purification.[16] Electrolysis of water leads to the formation of O_2 and H_2 bubbles on the surface of the electrodes. Bubble accumulation on the electrodes and subsequently in other parts of the device leads to progressing electric-field distortion and diminishing quality of purification within the first several minutes of operation.[17,18] The regeneration of an FFE device requires complete bubble flush-out: a cumbersome and time-consuming process. The goal of this work was to find a solution for the problem of FFE instability caused by bubble accumulation, thereby permitting reliable steady-state operation without the distortion of electric field or separation quality. Solving the bubble-accumulation problem is pivotal to FFE integration with other micro-systems.[19]

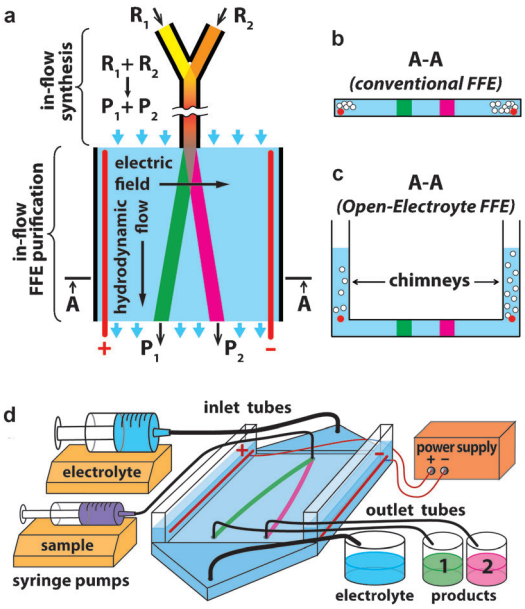

Figure 1. a) Schematic top view of an integrated system for continuous-flow microsynthesis and subsequent continuous-flow purification. The reactants, R_1 and R_2, generate products, P_1 and P_2, which are separated by FFE. A conceptual comparison of cross-sections (section A–A in panel (a)) in devices for conventional FFE (b) and our OEFFE (c). In OEFFE, bubbles (○) generated at the electrodes (red dot) are vented out of the device into the atmosphere through the chimneys. d) General overview of an OEFFE device.

The previous approaches to the problem of bubble accumulation in FFE devices could be split into three major categories: 1) a mechanical barrier preventing the entry of bubbles into the separation channel,[20] 2) separate electrode channels with fast flow for bubble removal,[21] and 3) chemical agents that inhibit gas generation and bubble growth.[22] While being useful, these measures only delay the accumulation of the deteriorating amount of bubbles. Bubbles still accumulate and prevent steady-state continuous separation. Because of bubble accumulation, electrical-current and sample-flow stability in FFE typically lasts for less than 0.5 h.[22] The longest operational time demonstrated for small-scale FFE is 2 h.[23]

This work was inspired by an insight that a solution to the bubble-accumulation problem could be achieved by breaking the principle of a closed FFE device. Our logic was simple. Bubble removal into the atmosphere could be easy and natural if the electrolyte above the electrodes was open to the atmosphere. Further, engineering the "open-concept" FFE device requires vertical chimneys to hold a column of electrolyte that hydrostatically balances the pressure inside the device. Since the Archimedes force pushes the gas upwards, bubble entry into the separation channel can be

[*] F. J. Agostino, Dr. L. T. Cherney, Dr. V. Galievsky, Prof. S. N. Krylov
Department of Chemistry and Centre for Research on Biomolecular Interactions, York University
4700 Keele Street, Toronto, Ontario M3J 1P3 (Canada)
E-mail: skrylov@yorku.ca

[**] We thank Natural Sciences and Engineering Research Council of Canada.

Supporting information for this article is available on the WWW under http://dx.doi.org/10.1002/anie.201300104.

completely prevented by placing the electrodes in the chimneys above the level of the separation channel. We term this approach open-electrolyte FFE (OEFFE). Figure 1 schematically illustrates the differences between the classical planar FFE device (Figure 1 b) and an OEFFE device with chimneys (Figure 1 c). Ideally, the setup should be designed to include a way to collect sample fractions after being purified, and also to collect and potentially recycle the electrolyte. The general schematic of an OEFFE device is illustrated in Figure 1 d, and a detailed drawing is shown in Figure S1.

We first attempted to test OEFFE experimentally by adding the chimneys to the previously developed and optimized planar device.[24] The parts of the device were made of poly(methyl methacrylate) by robotic micro-milling and bonded together with dichloromethane. Despite the apparent simplicity of OEFFE, all of our initial attempts to construct a functional OEFFE device had failed. The flow through the separation channel was not uniform (streamlines were significantly curved) and always diverted from the separation channel into the chimneys (Figure 2 a). Experimental variation of the device geometry and operation conditions proved to be a slow and inefficient way of solving this problem.

Difficulties of experimental optimization of a real OEFFE device prompted us to design a virtual OEFFE device for its theoretical optimization before building a real device. The virtual OEFFE device was constructed with COMSOL Multiphysics 4.3a commercial software (COMSOL Group, Palo Alto, CA), a program which allows complete modeling

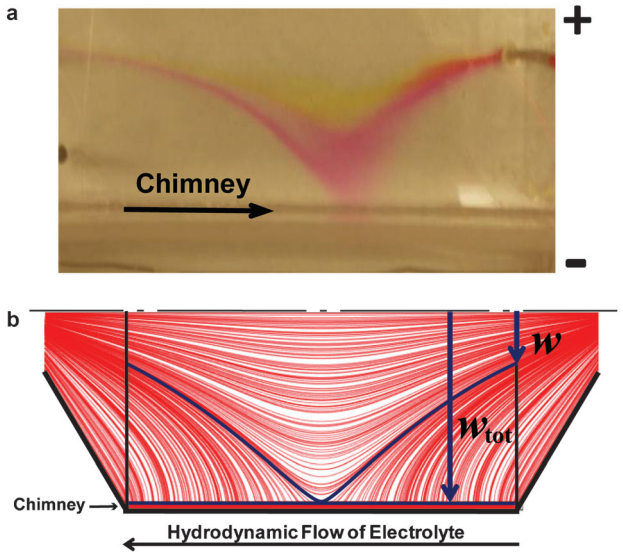

Figure 2. Flow non-uniformity in non-optimized OEFFE device: a) real and b) virtual. The hydrodynamic flow rate in both the virtual and real devices was 5 mL min^{-1}. A mixture of 2 dyes (fluorescein and rhodamine B) was continuously injected in the real device at a rate of 4 μL min^{-1}. The electric field was 50.0 V cm^{-1}. In the non-optimized device, the dye streams were deflected into the chimneys, diminishing the quality of separation. The virtual model illustrates the definition of the optimization parameter w/w_{tot} (see details in the text). Maximizing this parameter leads to a more uniform flow across the width of the separation channel. The value of w/w_{tot} in this example is 0.26 while its theoretical maximum is 1. All parts show halves of the devices.

of the flows within the device. The COMSOL simulation uses 3D modeling and presents the streamline patterns from a top-view for clarity of demonstration. The Experimental Section highlights experimental parameters, equations, meshing conditions, and boundary conditions used. To reduce computation time, we simulated a half of the symmetrical device (Figure S2 shows simulation of the full device).

We studied a number of virtual devices mimicking the initial experimental devices which had non-uniform flows. The flows in the virtual devices were similar to the ones in the real devices (see example in Figure 2), which confirmed the accuracy of the virtual device operation. After this test, we could use the virtual OEFFE device for the optimization of its geometry. The goal was to achieve as uniform flow in the separation channel as possible. A numerical parameter used to characterize flow uniformity was a ratio w/w_{tot} (see Figure 2 b). Where, w is the width of the part of the separation channel entry gate which incorporates only streamlines that do not leave the main part of the separation channel and w_{tot} is the total width of the entry gate that does not include chimneys. A greater value of w/w_{tot} corresponds to a more uniform flow, and, thus, optimization was done through maximizing w/w_{tot}.

Our optimization procedure required the identification of geometric parameters that could be varied to maximize w/w_{tot}. It is already known that the correct geometry of triangular electrolyte-entrance and electrolyte-exit reservoirs (located, respectively, at the top and bottom of an FFE device, see Figure S1) are essential for establishing parallel flow streamlines through a small-scale FFE device without chimneys.[24] The separation channel thickness was set to 200 μm, which was the minimum value to achieve reproducible FFE results using our fabrication technique.[25] In such a case, the movement of a viscous fluid in a shallow separation channel is possible when a pressure difference is applied between the input and output, that is, there is a pressure decrease along the flow. However, in OEFFE, the introduction of chimneys, which are open to the atmosphere, provide isobaric pressure along the entire boundary with the separation channel. Thus, there also exist significant pressure changes in a direction perpendicular to the boundary, and, as a result, undesirable fluid transferring occurs between the separation channel and chimneys.

We first attempted to optimize the chimney width, (Figure 3 a) and our simulations showed that decreasing the width of the chimneys increases w/w_{tot} to a value of 0.54 when the chimney is 0.5 mm wide (Figure 3 b). Our limitation, however, is that the chimney width cannot be smaller than the diameter of the electrode (0.75 mm) and in reality should allow extra space for bubble escape. We, therefore, set the minimum chimney width to 1.5 mm ($w/w_{tot} = 0.44$). This width is not sufficiently small to achieve a uniform flow (Figure 3 c).

To further optimize flow uniformity we needed a new feature in the device that could significantly decrease the undesirable pressure gradient across the separation channel. We suggested that deep and narrow sacrificial channels, parallel to the separation channel and located between the separation channel and the chimneys, could help to solve the problem (Figure 4 a). Explaining the design and implementa-

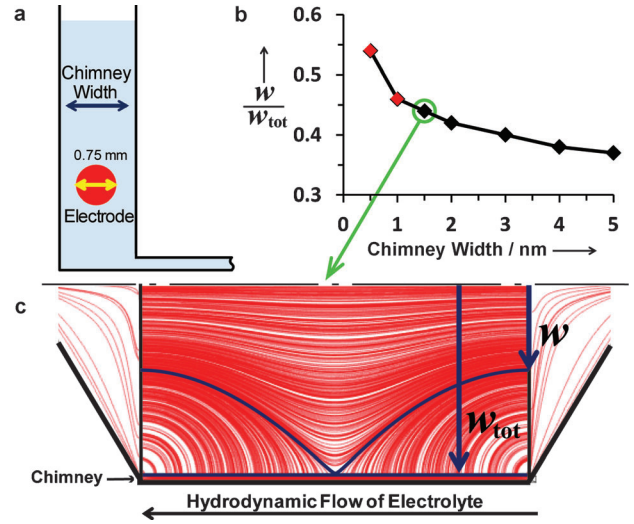

Figure 3. Theoretical optimization of flow uniformity with respect to chimney width. a) Schematic of the chimney, highlighting the chimney width in relation to the electrode width. b) Dependence of flow uniformity on the width of the chimney, where (red ◆) identifies chimney widths that are unfeasible because of the electrode diameter being a physical limitation. c) Theoretical product of optimizing the flow by decreasing the chimney width to 1.5 mm. The resultant w/w_{tot} is equal to 0.44.

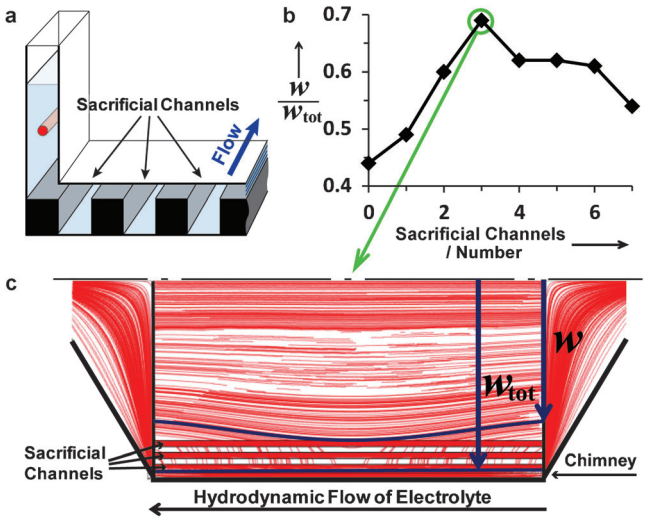

Figure 4. Theoretical optimization of hydrodynamic flow uniformity with respect to the number of sacrificial channels. a) Schematic of sacrificial channels built into the separation channel. b) Dependence of uniform flow on the number of sacrificial channels constructed in the separation channel. The optimal number of sacrificial channels is 3, with a $w/w_{tot} = 0.69$. c) Improvement in flow uniformity after 3 sacrificial channels are introduced.

tion of sacrificial channels follows this logic: the sacrificial channel has a much larger volumetric flow rate than the separation channel, because of its greater depth, and as a result the flow within it is less likely to diverge into the chimneys. Additionally, the influence of the isobaric boundaries in the chimneys on the fluid dynamics in the separation channel can be further reduced. We decided to explore the use of multiple parallel sacrificial channels, separated by narrow spaces, which could attenuate the fluid exchange between adjacent sacrificial channels (Figure S3). As a result, we thought that sacrificial channels could prevent the flow divergence towards the chimneys.

We first introduced a single sacrificial channel and found that our hypothesis was correct—it improved flow uniformity. We then optimized its width and depth (Figure S4). As a result, we limited both the width and depth of the sacrificial channel to 1.5 mm which generated a marginal increase in the value of w/w_{tot} from 0.44 to 0.49. In an attempt to further improve flow uniformity, we explored the effect of multiple sacrificial channels. To facilitate the faster optimization process we assumed that: 1) all sacrificial channel have the same dimensions and 2) the distances between them are equal. We discovered that the dependence of w/w_{tot} on the number of sacrificial channels displays a maximum when the number of channels was equal to 3 (Figure 4b). Three sacrificial channels allowed us to achieve $w/w_{tot} = 0.69$ (Figure 4c). While the width of the sacrificial channel was an important optimization parameter (Figure S4b), one wide channel did not have the same effect as three narrow channels (Figure S5). We also tested our final theoretical model for its robustness with respect to separation channel depth (Figure S6) and hydrodynamic flow rates (Figure S7). These simulations were performed to ensure that any variability that might be caused by machining or operational precision did not significantly affect the device performance. In both cases, the optimized OEFFE proved to be robust.

The hard copy of the theoretically optimized OEFFE device was then prepared using the approach described above. The device was first tested for flow uniformity. The sample flow had relatively straight streamlines suggesting that the optimization was successful, and once again proving the accuracy of the virtual device operation. We then tested the device for bubble formation. Bubbles formed on the electrodes and dislodged from them when they reached the critical size. Bubbles vented out into the atmosphere and did not enter the separation channel. Under such conditions the electric current showed no drift during a 12 h period of continuous work, thus, suggesting its steady-state bubble removal.

Our final test was for stability of electrophoretic separation. A mixture of three dyes (rhodamine B, rhodamine 6G, and fluorescein) was continuously injected by a syringe pump that provided uninterrupted injection for 12 h. The stability of separation was judged by the steadiness of the three streamlines. No deterioration in separation quality was noticed (Figure 5), suggesting the steady-state operation of the device. On the other hand, only negligible widening of streamlines during their passage through the separation channel suggests minimal contribution from multiple sources of band-broadening such as diffusion, injection bandwidth, convection, and hydrodynamic broadening. Injection bandwidth is limited by simply decreasing the diameter of the sample inlet. Decreasing the depth of the separation channel reduces convective and hydrodynamic broadening.[19] Therefore, not only can this device support steady-state continuous separation, but it also satisfies the general requirement of negligible band broadening.

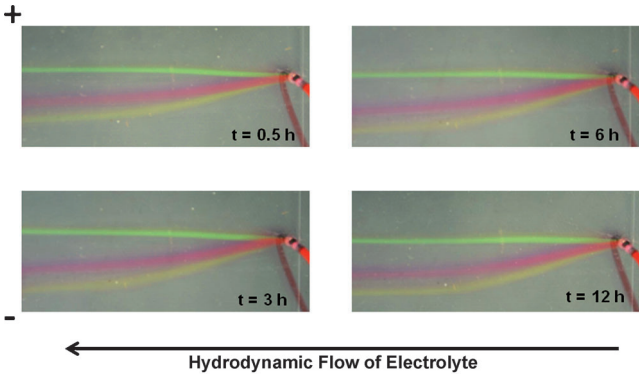

Figure 5. Steady-state continuous separation of 250 mM fluorescein (green), 250 mM rhodamine B (pink), and 250 mM rhodamine 6G (yellow) by OEFFE. An electric field of 50.0 $V cm^{-1}$ was applied across the chip for a 12 h period. The hydrodynamic flow rate of the electrolyte was (5.00 ± 0.5) $mL min^{-1}$. A mixture of the three dyes was introduced at a flow rate of (4.00 ± 0.01) $\mu L min^{-1}$. Current reading was stable at (25 ± 1) mA. Removing the bubbles from the OEFFE device prevented electric field distortion and supported its steady-state separation with constant quality of separation.

To conclude, we have successfully demonstrated steady-state small-scale continuous separation. OEFFE ultimately solves the problem of the deterioration of separation quality over time by preventing the accumulation of bubbles in the device. The introduction of chimneys caused non-uniformity in hydrodynamic flow, which was circumvented by novel features called sacrificial channels. With the assistance of COMSOL simulations, we found the appropriate geometries of the chimneys and sacrificial channels to achieve acceptable flow uniformity. According to our results, flow uniformity can be further optimized and will be evaluated in future studies. Although we have only developed an OEFFE prototype in plastic, it will be prudent to create analogues in solvent resistant material, to expand the scope of solvents and analytes for which OEFFE is suitable. It should be noted that classical electrophoresis is applicable for separation of analytes with different charge/size ratios. Modifications of classical electrophoresis have been developed for the separation of uncharged species. Micellar electrokinetic chromatography uses charged surfactants, at concentrations that are greater than critical micelle concentration, to separate uncharged species with different hydrophobicities.[26–28] Dielectrophoresis, another example, uses non-uniform electric fields to separate uncharged species with different dipole moments.[29,30] Achieving steady-state continuous separation, with a technologically simple solution, will stimulate efforts aiming at practical integration of continuous microsynthesis with continuous purification.

Experimental Section

To simulate OEFFE devices we used COMSOL. The steady state Navier-Stokes equation was used for the computations, with the condition of non-compressible flow. The laminar flow physics model was chosen and we input a flow rate of 5 $mL min^{-1}$ into the electrolyte inlet (shown in Figure S1). The boundary conditions include: no-slip walls; laminar inflow at the inlet; and no viscous stress at the outlet. The meshing geometry used was tetrahedral, with a fine size in areas of large volume (exit and entrance reservoirs), and extremely fine geometry in narrow regions (separation channel, sacrificial channels, and chimneys). Default stabilization conditions (with a tuning parameter $C_k = 1$) were selected: streamline diffusion and crosswind diffusion. 3D models were prepared to fully capture the flow system in only one half of the device to facilitate simulation time. We have included in the Supporting Information the optimized COMSOL file thoroughly detailing our simulation strategy. The mathematical model includes the following relations. Laminar flow equations inside the device:

$$\rho(v\nabla)v = \nabla\{-pI + \mu[\nabla v + (\nabla v)^T]\} \quad (1)$$

$$\rho\nabla v = 0 \quad (2)$$

Wall boundary condition:

$$v = 0 \quad (3)$$

Inlet condition:

$$L_{entr}\nabla_t\{-p_{enter}I + \mu[\nabla_t v + (\nabla_t v)^T]\} = -p_{enter}n \quad (4)$$

$$\nabla_t v = 0 \quad (5)$$

Outlet condition:

$$p = p_0, \quad [\mu(\nabla v + (\nabla v)^T)]n = 0 \quad (6)$$

Symmetry conditions at the symmetry plane $x = 0$:

$$vn = 0, \quad K - (Kn)n = 0 \quad (7)$$

$$K = [\mu(\nabla v + (\nabla v)^T)]n \quad (8)$$

Where, ρ and μ are density and viscosity of the liquid; v and p are the velocity and pressure; K is the viscous force at the symmetry plane; p_{enter} and p_0 are the pressures at the inlet and outlet, respectively; L_{entr} is a parameter used by COMSOL in the inlet condition, I is the unit tensor; n is the normal to the walls or to the symmetry plane; the superscript T denotes a transpose matrix.

All reagents were purchased from Sigma Aldrich, unless otherwise mentioned. OEFFE prototypes were fabricated from poly(-methyl methacrylate) stock material using a MDX-540 robotic milling machine. The optimized cutting speeds for the end mills have already been described in full detail.[24] Refer to Supporting Information (Experimental Details) for full details of OEFFE assembly.

An electrolyte solution was prepared with 25 mM 4-(2-hydroxyethyl)-1-piperazineethanesulfonic acid (HEPES) (99.5%) and was adjusted with 10 M NaOH to pH 7.5. Triton X-100 (0.001 [w/v]) was added to it and the mixture was deoxygenated by bubbling with N_2 overnight. A sample containing 250 mM of each fluorescein, rhodamine B, and rhodamine 6G, was prepared in this electrolyte. A separate 10% EtOH solution was used as a primary wash solution to wet the surface of the OEFFE device. All solutions were prepared using de-ionized H_2O.

The hydrodynamic flow of the electrolyte was driven by a continuous flow syringe pump system (New Era Pump System Inc, Farmingdale, NY, USA). The electrolyte flow rate in the experiment highlighted herein (5.00 ± 0.05) $mL min^{-1}$. A separate syringe pump (Harvard Apparatus Pump II, Saint-Laurent, Canada) was used to introduce the sample at a flow rate of (4.00 ± 0.01) $\mu L min^{-1}$. Experiments were carried out at room temperature. The OEFFE device was placed on top of metal blocks, which were in contact with ice packs, to help prevent overheating.

The voltage applied to the electrodes was 500 V, which corresponds to an electric field strength of 50.0 $V cm^{-1}$ inside the

separation channel. For 12 h, the current was recorded and digital pictures (Nikon 7000) were taken to monitor the sample separation quality in the presence of an electric field.

Received: January 7, 2013
Revised: February 25, 2013
Published online: June 10, 2013
Publication delayed at the request of the author

Keywords: bubbles · continuous flow microsynthesis · free-flow electrophoresis · open-electrolyte · separation techniques

[1] J. R. Burns, C. Ramshaw, *Chem. Eng. Res. Des.* **1999**, *77*, 206 – 211.
[2] C. Wiles, P. Watts, S. J. Haswell, E. Pombo-Villar, *Tetrahedron* **2005**, *61*, 10757 – 10773.
[3] R. D. Chambers, M. A. Fox, G. Sandford, *Lab Chip* **2005**, *5*, 1132 – 1139.
[4] E. Comer, M. G. Organ, *J. Am. Chem. Soc.* **2005**, *127*, 8160 – 8167.
[5] Y. Wada, M. A. Schmidt, K. F. Jensen, *Ind. Eng. Chem. Res.* **2006**, *45*, 8036 – 8042.
[6] N. Kockmann, D. M. Roberge, *Chem. Eng. Technol.* **2009**, *32*, 1682 – 1694.
[7] R. Schenk, V. Hessel, C. Hofmann, J. Kiss, H. Löwe, A. Ziogas, *Chem. Eng. J.* **2004**, *101*, 421 – 429.
[8] F. Ullah, T. Samarakoon, A. Rolfe, R. D. Kurtz, P. R. Hanson, M. G. Organ, *Chem. Eur. J.* **2010**, *16*, 10959 – 10962.
[9] O. C. Okafor, S. Tadepalli, G. Tampy, A. Lawal, *Ind. Eng. Chem. Res.* **2010**, *49*, 5549 – 5560.
[10] S.-A. Leung, R. F. Winkle, R. C. R. Wootton, A. J. deMello, *Analyst* **2005**, *130*, 46 – 51.
[11] T. Hatakeyama, D. L. Chen, R. F. Ismagilov, *J. Am. Chem. Soc.* **2006**, *128*, 2518 – 2519.
[12] C. Wiles, P. Watts, *Eur. J. Org. Chem.* **2008**, 1655 – 1671.
[13] K. Hannig, H. Wirth, B.-H. Meyer, K. Zeiller, *Hoppe-Seyler's Z. Physiol. Chem.* **1975**, 1209 – 1223.
[14] K. Hannig, H. Wirth, R. K. Schindler, K. Spiegel, *Hoppe-Seyler's Z. Physiol. Chem.* **1977**, *358*, 753 – 764.
[15] D. E. Raymond, A. Manz, H. M. Widmer, *Anal. Chem.* **1994**, *66*, 2858 – 2865.
[16] A. Persat, M. E. Suss, J. G. Santiago, *Lab Chip* **2009**, *9*, 2454 – 2469.
[17] T. Revermann, S. Gotz, J. Kunnemeyer, U. Karst, *Analyst* **2008**, *133*, 167 – 174.
[18] H. Vogt, *J. Appl. Electrochem.* **1983**, *13*, 87 – 88.
[19] R. Turgeon, M. T. Bowser, *Anal. Bioanal. Chem.* **2009**, *394*, 187 – 198.
[20] D. E. Raymond, A. Manz, H. M. Widmer, *Anal. Chem.* **1996**, *68*, 2515 – 2522.
[21] B. R. Fonslow, V. H. Barocas, M. T. Bowser, *Anal. Chem.* **2006**, *78*, 5369 – 5374.
[22] D. Kohlheyer, J. C. T. Eijkel, S. Schlautmann, A. van den Berg, R. B. M. Schasfoort, *Anal. Chem.* **2008**, *80*, 4111 – 4118.
[23] N. Frost, M. T. Bowser, *Lab Chip* **2010**, *10*, 1231 – 1236.
[24] B. R. Fonslow, M. T. Bowser, *Anal. Chem.* **2008**, *80*, 3182 – 3189.
[25] F. J. Agostino, C. J. Evenhuis, S. N. Krylov, *J. Sep. Sci.* **2011**, *34*, 556 – 564.
[26] S. Terabe, K. Otsuka, T. Ando, *Anal. Chem.* **1985**, *57*, 834 – 841.
[27] S. Terabe, *J. .Pharm. .Biomed. Anal.* **1992**, *10*, 705 – 715.
[28] S. A. A. Rizvi, D. P. Do, A. M. Saleh, *Cent. Eur. J. Chem.* **2011**, *2*, 276 – 281.
[29] P. R. C. Gascoyne, J. Vykoukal, *Electrophoresis* **2002**, *23*, 1973 – 1983.
[30] M. P. Hughes, *Electrophoresis* **2002**, *23*, 2569 – 2582.